

## Article

# An Experimental and Numerical Investigation of a Novel 3D Printed Sandwich Material for Motorsport Applications

Harland, Daniel John, Al Shaer, Ahmad Wael and Brooks, Hadley Laurence

Available at <http://clock.uclan.ac.uk/29867/>

*Harland, Daniel John ORCID: 0000-0002-7967-7537, Al Shaer, Ahmad Wael ORCID: 0000-0002-5031-8493 and Brooks, Hadley Laurence ORCID: 0000-0001-9289-5291 (2019) An Experimental and Numerical Investigation of a Novel 3D Printed Sandwich Material for Motorsport Applications. Procedia Manufacturing, 36 . pp. 11-18.*

It is advisable to refer to the publisher's version if you intend to cite from the work.  
<http://dx.doi.org/10.1016/j.promfg.2019.08.003>

For more information about UCLan's research in this area go to  
<http://www.uclan.ac.uk/researchgroups/> and search for <name of research Group>.

For information about Research generally at UCLan please go to  
<http://www.uclan.ac.uk/research/>

All outputs in CLoK are protected by Intellectual Property Rights law, including Copyright law. Copyright, IPR and Moral Rights for the works on this site are retained by the individual authors and/or other copyright owners. Terms and conditions for use of this material are defined in the [policies](#) page.

17th Nordic Laser Material Processing Conference (NOLAMP17), 27 – 29 August 2019

## An Experimental and Numerical Investigation of a Novel 3D Printed Sandwich Material for Motorsport Applications

Daniel Harland<sup>a</sup>, Ahmad W. Alshaer<sup>a,\*</sup>, Hadley Brooks<sup>a</sup>

<sup>a</sup>*School of Engineering, University of Central Lancashire, Fylde Street, Preston, PR1 2HE, The UK*

---

### Abstract

In this paper, a novel 3-D printed core material is developed to investigate the cores structures' strength and stiffness under bending. Using powder bed fusion, Nylon PA12 structures have been produced and CFRP skin material has been applied to the 3D printed cores. The three-point bending behaviour and failure of the developed material are compared to the commonly used Al honeycomb structure. The 3D printed re-entrant structure supported the largest load among all tested cores and showed a superior stiffness in comparison to Al honeycomb cores although the latter achieved the maximum strength and stiffness to weight ratio. Additionally, a numerical 3D FEA model has been developed to investigate the re-entrant core's nonlinear mechanical behaviour under loading. The numerical results were in a very good agreement with the experiments in terms of the loading force, plastic deformation and the failure mode.

© 2019 The Authors. Published by Elsevier B.V.

Peer-review under responsibility of the scientific committee of the 17th Nordic Laser Material Processing Conference.

**Keywords:** Sandwich Materials; SLS; 3D printing; Honeycomb; Reentrant

---

### 1. Main text

Sandwich composite materials are widely used in structural engineering, namely in advanced engineering products where greater durability and reduced weight are imperative. Due to the need for light-weight structures for the motorsports and aerospace industry, foam has been ideal for forming the core's material [1]. However, such materials have a bending-dominated deformation and can be limited when scaled. Therefore, other alternatives have been proposed with better mechanical properties such as cellular honeycomb cores, lattice truss, and the re-entrant

---

\* Corresponding author. Tel.: +44 (0) 1772 89 3279.

E-mail address: [awalshaer@uclan.ac.uk](mailto:awalshaer@uclan.ac.uk)

honeycombs [2]. A number of experimental and numerical studies confirmed the improved performance of the honeycomb and other corrugated structures under bending and impact [3–6]. However, the improvement of their performance can be limited to the increase of the cells' dimensions which increases the structure's weight and may need thicker skins for a better bending stresses resistance [7]. Those limitations opened the door for 3D printed complex structure to be used for a better performance. Research has been done on continuous fibre composite corrugated PLA structures with face sheets whose compressive resistance was evaluated [8]. Although the structures showed good compressive strength, only small samples of one type was tested. Moreover, the method used two different materials, namely PLA and Kevlar fibres, which may raise issues with the process optimisation and maintaining its consistency. Sarvestani *et al.* [9] used material extrusion to produce PLA 3D printed structures and studied their impact resistance using square samples and proposed an analytical model to describe the impact energy absorbance function. In addition to the fact that the authors only tested square-shaped cores whose response may be different when formed in a non-uniform shape, extruded PLA is very stiff in comparison to Nylon or rubber which may be more ideal for impact absorption applications. In a relevant research [10, 11] a couple of 3D printed core structures including the honeycomb and other auxetic structures were investigated and their resistance to compression was evaluated. Although the proposed 3D printed structures showed a good compression resistance, their performance was not compared to the currently available cores such as aluminium honeycomb cores, and only a relative comparison among the 3D printed structures was made. Moreover, the tested 3D printed structures formed only one or a few cells that were supported by 3D printed walls. The behaviour captured in those investigations may not show the interaction of the large number of cells when they are loaded as a unit, and hence may not resemble the real-life loading environment. In a different research [12], a larger number of cells with similar structure were numerically investigated using FEA but the numerical results were not validated against any experimental data. Li T. and Wang L. [13] investigated the bending strength of a sandwich material made of an acrylic-based photopolymer and the bending test was performed on a sample with only 10 mm beam width and CFRP skins made of 16 carbon fibre sheets. The proposed samples were not compared to any commercially available cores such as Al honeycomb, and their stiffness was found to be relatively low (2.6 to 33 N/mm) and may not support all industrial applications that require high stiffness. This is due to the nature of the used material (Verowhite) which has low stiffness and does not maintain its properties above 50°C. Applying such materials in areas close to the engine in motorsports vehicles, where operating temperatures may be higher than that, can be a challenge.

It can be seen from the literature that this area of research is still in its infancy and a full understanding of the 3D printing core's behaviour is still required. In this paper, the bending strength and stiffness of two different 3D printed cores were investigated and compared against a common and commercially used Al honeycomb core structure. Moreover, the samples created were in relatively large scale, which is more industrially relevant, and a full FEA model was created to understand the behaviour of one of the 3D printed cores.

## 2. Materials and Experimental Setup

The face composite sheets were fabricated using carbon fibre 2/2 Twill 3K 240g sheets and EL2 Epoxy Laminating Resin which was mixed with AT30 slow Epoxy hardener at 100:30 ratio to achieve a final sheet thickness of 3 mm. The samples were cold cured at room temperature to prevent any change of the 3D printed cores properties. The sheets were applied to the 3D printed and aluminium cores using the same type of epoxy. The aluminium cores were made of AA3003 alloy with a wall thickness of 0.5 mm while the 3D printed cores were made of EOS PA2200 powder (also known as Nylon PA12) which were laser sintered on a FORMIGA P110. The process parameters are given in Table 1. The honeycomb and re-entrant cell geometry is depicted in Fig. 1 (a and b) and the overall dimensions of the samples are 150x75x19 mm<sup>3</sup>. The three-point bending tests were carried out using a Testometric FS500CT 500kN machine with 20 mm/min loading speed, 20 N preload and a maximum deflection limit of 20 mm.

## 3. Numerical model

The simulations were run on Ansys Workbench 14.5 with more than 300,000 tetrahedral elements and on a system equipped with an Intel XEON E3-1230 V2 3.3 GHz processor, 16 GB RAM and a Windows 10 operating system, and

16 hours and 120 sec computational and physical time were used respectively.

A 3-D model was created to simulate the actual re-entrant core and its performance was evaluated by lowering the loading pin by a 20 mm distance at a 20 mm/min speed. The supporting pins were fixed, and the reaction forces, stress, strain and deflection were recorded. A frictionless contact was set between the pins and the core.

Table 1. Process parameters and Nylon PA2200 material's properties [14, 15]

Process Parameters		Material Properties	
Laser Type	CO2 (10.6 $\mu\text{m}$ )	Bulk Density [ $\text{g}/\text{cm}^3$ ]	0.45
Laser Power [W]	30	Density for laser sintered part [ $\text{g}/\text{cm}^3$ ]	0.93
Scanning Speed [m/s]	5	Ave. Particle size [ $\mu\text{m}$ ]	56
Layer Height [mm]	0.1	Al Honeycomb weight [g]	100.36
Scanning Direction	Y	PA12 Honeycomb weight [g]	128.8
Processing Temp [ $^{\circ}\text{C}$ ]	170	PA12 Re-entrant weight [g]	170.9

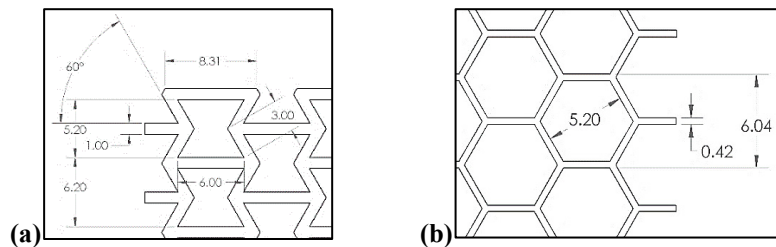


Fig. 1. Dimensions of the 3D printed cores' cells (a) the Re-entrant (b) the Honeycomb.

#### 4. Results and discussion

The fabricated samples were tested using three points bending test to evaluate the bending strength, strain and stiffness of the samples. Figure 2 shows the deformed samples and some key dimensions and features at the end of the bending test.

The distortion of the Al core is evident in Fig. 2 which shows a large deformation at the point of loading (the centre) and less distortion towards the right-hand side where the composite face delamination took place. Additionally, the top face of the sample is cracked in half when the maximum strain was reached.

In Fig. 2, the 3D printed honeycomb core's failure occurs due to the brittle fracture at the centre where the crack propagated across the entire sample. The in-plane shear forces developed in the adhesive material induced the separation of the bottom face on the right-hand side. The compressive and tensile forces at the panel's top and bottom faces respectively forms a couple that causes shear stresses to develop in the adhesive material until they exceed the joint shear strength, leading to delamination.

Similar failure behaviour can be observed in the 3D printed re-entrant cores although the shear stresses developed at the bottom face/core interface separates the two at the weakest location in the adhesive joint which may contain some defects produced by the manual fabricating of the sandwiches.

##### 4.1 Strength and Deformation

The relationships between the force and displacement and the stress versus strain are presented in Fig. 3 and a significant variation in the maximum load and displacement for the different samples can be seen. It can be derived from this Fig. that the Al cores start to yield at about 3% strain (approx. 3 mm displacement) causing the force to rise until the maximum value of about 7000 N is reached. After that, the force drops until it stabilises for a considerable time until the sandwich fails. The drop of the force/stress is caused by the large deformation of the core's cells until

the composite skins start to take over the load until break. This behaviour is entirely distinct from that of the 3D printed cores which behaved in a brittle manner. Their yielding curve consisted of two ramps which represent the core's and the skin's strength curve respectively. The large drop in force in the 3D printed core's curves occurs when the cores break, and the composite skins solely start to support the load until they fail.

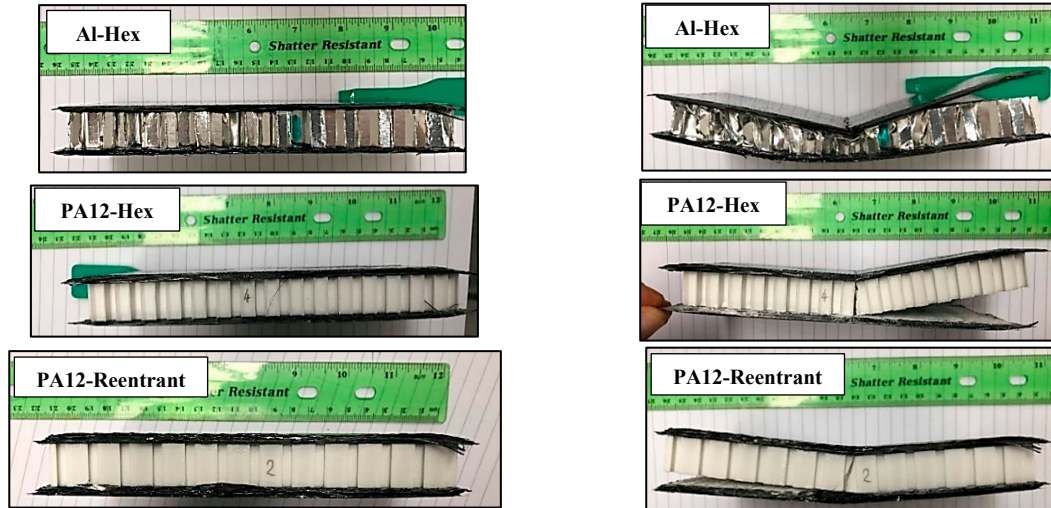


Fig. 2. Fabricated sandwiches before (left) and after (right) the bending test.

It can be seen from Fig. 3 that the 3D printed re-entrant core supported the maximum load of more than 10 kN in comparison to the Al and Nylon honeycomb cores which supported 7100 N and 5731 N respectively. This behaviour can be related to the negative Poisson ratio associated with the re-entrant structures which promotes a better resistance to deformation under compression [11].

The aluminium honeycomb core experienced the maximum deflection of about 21 mm compared to the 3D printed PA12 cores. The 3D printed honeycomb core deflected slightly larger than the re-entrant core by about 3 mm, which equals a strain increase by about 0.029 mm/mm. This difference in elongation under load is expected due to the significant difference in the ductility of the two materials since Al3003 alloy achieves 25% elongation at break while PA12 only achieves only about 5-7% [16].

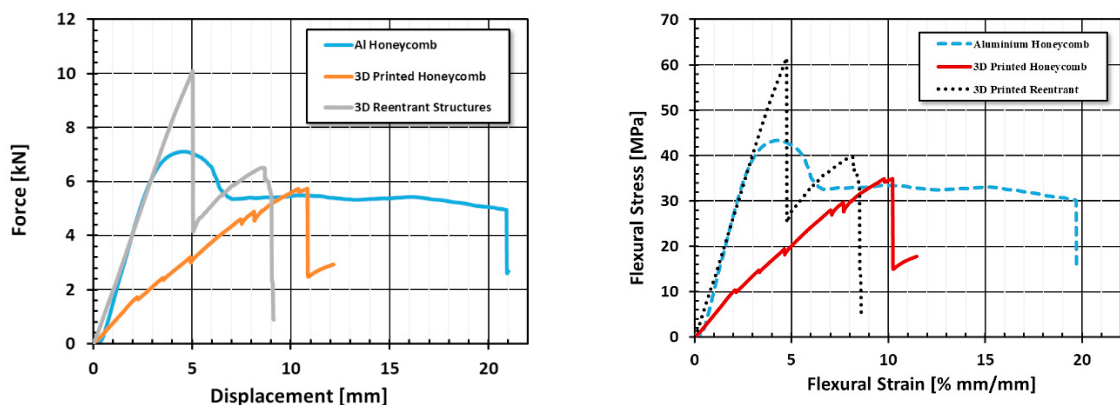


Fig. 3. Change of the load with displacement (left) the Flexural stress change with strain (right).

As shown in Fig. 3, both core materials show similar trend in the Stress-Strain graph. The maximum flexural stress achieved by the re-entrant cores reached more than 60 MPa at just less than 5% strain value. This value is larger than

the PA12 core's strength without the composite faces which will be discussed later sections in this paper. It is pertinent to mention that the “telegraph-signal” shape seen in the 3D printed honeycomb strength curve can be related to the failure of some of the carbon fibres which are under tension in the lower composite face of the sandwich [17]. The use of carbon fibres sheets with larger number of fibres in the single tow (6k, 12k sheets) may increase the strength of the face sheets and hence enhance the sandwich performance but this will affect the sandwich weight.

It was observed, as shown in Fig. 3, that the Al core was the toughest (largest area under the curve) and possibly the most damage tolerant compared to other cores. Moreover, 3D printed honeycomb core gave the least flexural strength, modulus and stiffness while the re-entrant achieved the maximum values in both the strength and stiffness as shown in Fig. 4. In addition to the best strength recorded of 61 MPa (41% more than the Al core), the re-entrant core achieved about 29% increase in the stiffness although it achieved a marginally smaller flexural modulus. This can be explained by the fact that Al core started yielding at smaller stress and strain than the re-entrant core which maintained its structural integrity until brittle failure occurred. Aluminium yielding made the sandwich core less rigid and caused the deflection to increase to a larger magnitude than that seen in the 3D printed core.

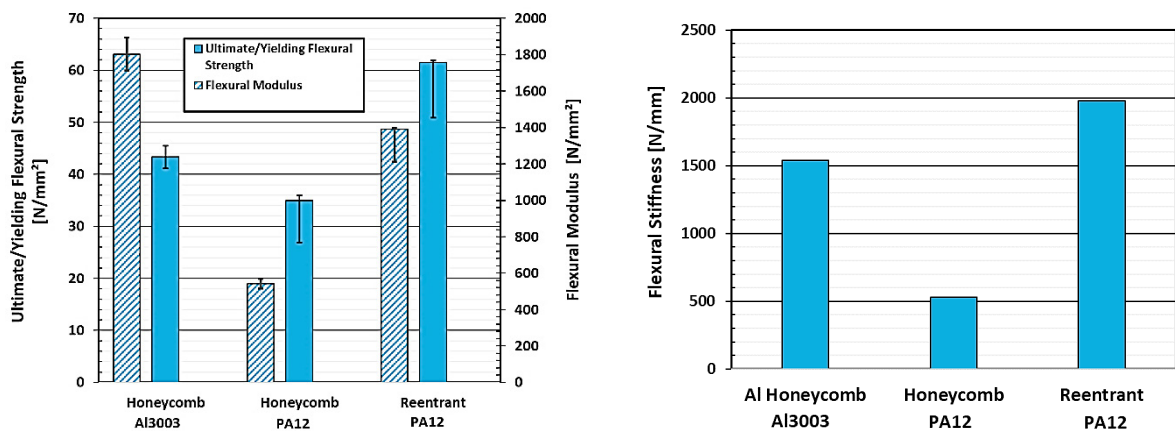


Fig. 4. Sandwiches maximum flexural strength (left) and their flexural stiffness (right).

To compare the different sandwich's performance for weight critical applications, the values of the strength and the stiffness were normalised using the sandwich weights as plotted in Fig. 5. It can clearly be concluded that the Al cores have the highest flexural strength, modulus and stiffness to weight ratio among all other cores while the 3D printed honeycomb cores have the least normalised values. This trend is related to the weight of the 3D printed cores which is currently 30-70% higher than Al cores. However, the weight can significantly be reduced using a variable resolution (cell size) across the core as well as reducing the cells' wall thickness which is currently 1 mm.

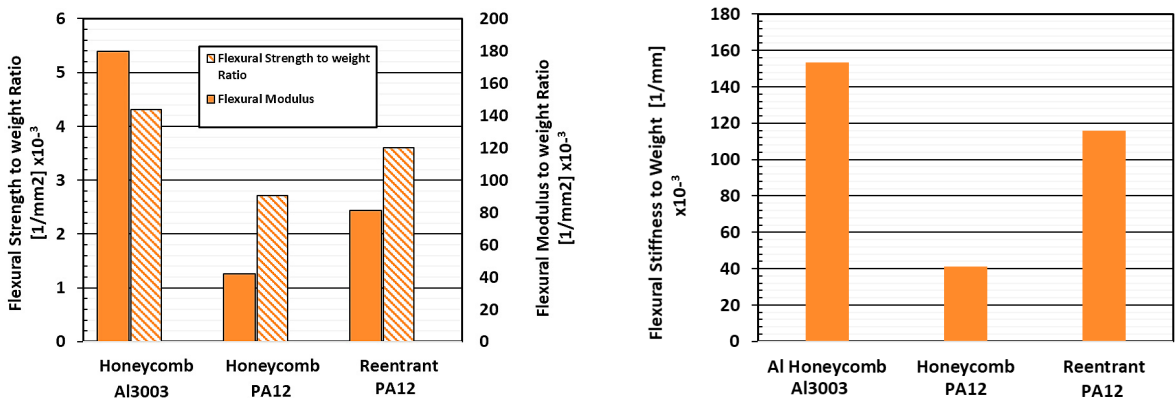


Fig. 5. Flexural strength to weight ratio (left) and flexural stiffness to weight ratio (right).

The variable resolution will not only reduce the weight, but it also strengthens the core where higher stresses are



expected and can also satisfy some design considerations such as the need for a pivot point to attach the sandwiches in a specific location in the vehicle's body. This variable resolution can be a challenge to be produced using aluminium or Nomex cores while it can be easily produced using 3D printing.

#### 4.2 Numerical results

Due to the superior performance of the re-entrant cores in terms of the strength and stiffness, a numerical study was carried out to further understand the behaviour of such structures. Figure 6 shows a 3D and sectioned view of the stresses developed in the core's material at 60 sec of loading when the maximum load was reached. In addition, the reaction forces are plotted against the displacement and the numerical values are compared to the experimental results carried out on 3D printed cores without face sheets as shown in Fig. 9.

It can be seen from Fig. 6 (a) and (b) that the maximum equivalent Von Mises stresses are concentrated on the top and the bottom layers of the core with a maximum value of about 50 MPa. The stresses values gradually decrease until they become zero at the far ends of the core where the bending moment is zero and at the neutral axis where the flexural stresses vanish. While the predominant compressive stresses at the top part causes the top edges of two cells to deform outwards causing a permeant set, the tensile stresses at the bottom which exceeds the material strength leads to the failure of the material. This behaviour correlates well to the experimental results which are presented in Figs 6 (c) and 7. It should be noted that although the FEA model currently developed does not account for the crack initiations and propagation and hence the material break is not shown in Fig. 6 (a) and (b). However, the failure can be numerically predicted when Von Mises stresses exceeds the materials ultimate strength.

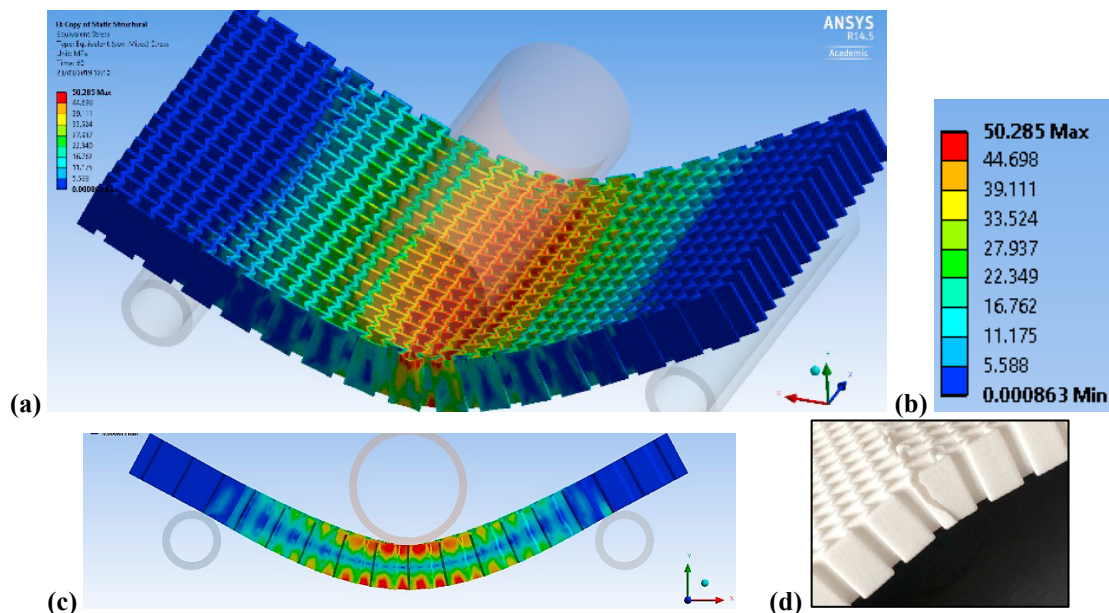


Fig. 6. FEA Von Mises stresses in a 3D printed re-entrant core (a) A dimetric view (b) Colour legend (c) A section view (d) Failure of the core at the bottom layers where the equivalent stress exceeded the material's strength.



Fig. 7. A qualitative comparison of the 3D printed re-entrant core failure shown by the plastic deformation of some of the cells between (a) the experimental and (b,c) FEA results.

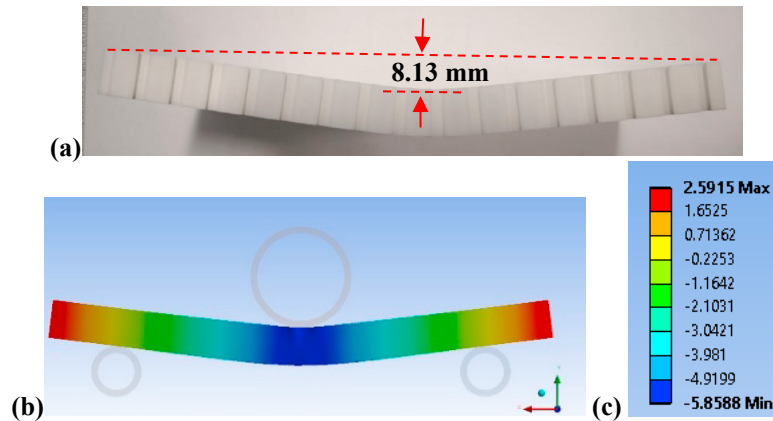


Fig. 8. (a) The experimental and (b) numerical plastic deformation observed in the re-entrant cores at 102 sec after the loading pin loses contact with the core (c) Colour legend for deformation shown in (b) in mm.

Moreover, the remaining plastic strain in the samples was also measured and compared to the model as shown in Fig. 8. The measured value of the permanent deflection of 8.13 mm agrees with the values predicted by the FEA model (8.45 mm) which is calculated by adding the min and max values of the displacement.

The change of the force as a function of displacement was also compared with the experimental results as shown in Fig. 9 (a). The two curves show a good agreement at the small displacement values and the FEA model shows a very similar behaviour to the experiment. However, the FEA maximum value of 608 N was higher than the experimental value by about 70 N which can be explained by the fact that the current FEA model assumes a perfect and homogenous properties for the PA12 material applied to the model, and it does not count for any weakly bonded or un-sintered micro powder particles that may be exist in the physical model. Hence, the difference in the force value may originate from some defects or irregularities the physical core during manufacturing process, which may lead to an earlier failure than that predicted in the FEA model. Moreover, the core's fracture that occurs in the experiment may release some of the stresses developed in the sandwich material and may lead to a smaller value of the reaction force at the end of the loading phase. This effect is absent in the FEA model since it does not take the material's fracture into consideration.

Finally, Fig. 9 (b) shows how Von Mises stress value increases in a linear fashion in the elastic region until plastic deformation take place and the stress becomes constant until the material's failure. It should be noted that the value of the Von Mises stress of about 50 MPa is larger than the materials ultimate strength of about 48 MPa, indicating that the materials failure happens.

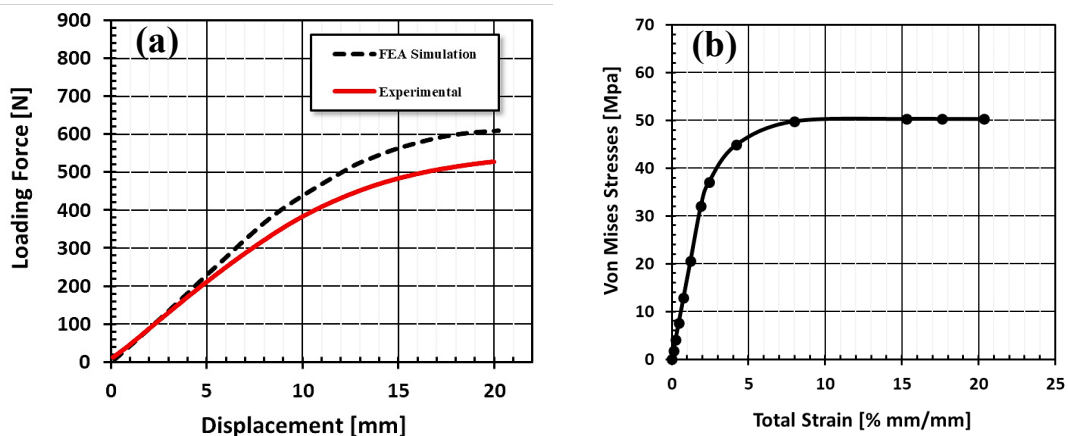


Fig. 9. (a) Force versus displacement (b) Stress/Strain numerical behaviour of the re-entrant core.



## 5. Conclusions

The strength and stiffness of two different 3D printed core structures were investigated and their performance was compared to a common Al honeycomb sandwich material used in aerospace and motorsports applications. Moreover, a numerical FEA model was created to further understand the behaviour of the re-entrant 3D printed cores since it achieved the best performance of all cores in terms of strength and stiffness. The following conclusions can be drawn from this work:

1. The 3D printed re-entrant cores supported higher loads and were stiffer than the Al honeycomb cores while the 3D printed honeycomb cores showed the poorest performance.
2. The Al core achieved the largest strength and stiffness to weight ratio that was higher than that of the re-entrant cores by about 44% and 29% respectively. However, this trend can be reversed by reducing the 3D printed cells' wall thickness (1 mm) and using the advantages of the 3D printing process as explained earlier.
3. The Al cores experienced large deformation in the core region before the face sheets failed, while the 3D printed cores showed minimal distortion before fracture.
4. The FEA model predicted the re-entrant cores failure which was validated against the experimental work. The Von Mises stress maximum value exceeded the material's strength of 48 MPa, and the permanent deflection of the core of about 8.13 mm was in an excellent correlation with the numerical value of 8.45 mm.

## References

1. Schaedler, T.A. and W.B. Carter, *Architected Cellular Materials*. Annual Review of Materials Research, 2016. **46**(1): p. 187-210.
2. Ashby, M., *Metal foams: a design guide*. 2000: Boston: Butterworth-Heinemann.
3. Burton, W.S. and A.K. Noor, *Assessment of continuum models for sandwich panel honeycomb cores*. Computer Methods in Applied Mechanics and Engineering, 1997. **145**(3): p. 341-360.
4. Rathbun, H.J., et al., *Performance of metallic honeycomb-core sandwich beams under shock loading*. International Journal of Solids and Structures, 2006. **43**(6): p. 1746-1763.
5. Petras, A. and M.P.F. Sutcliffe, *Failure mode maps for honeycomb sandwich panels*. Composite Structures, 1999. **44**(4): p. 237-252.
6. Buitrago, B.L., et al., *Modelling of composite sandwich structures with honeycomb core subjected to high-velocity impact*. Composite Structures, 2010. **92**(9): p. 2090-2096.
7. ALLEN, H.G., *Analysis and Design of Structural Sandwich Panels, A volume in The Commonwealth and International Library: Structures and Solid Body Mechanics Division*. 1969: Elsevier Ltd.
8. Hou, Z., et al., *3D printed continuous fibre reinforced composite corrugated structure*. Composite Structures, 2018. **184**: p. 1005-1010.
9. Yazdani Sarvestani, H., et al., *3D printed architected polymeric sandwich panels: Energy absorption and structural performance*. Composite Structures, 2018. **200**: p. 886-909.
10. Wu, Q., et al., *Mechanical properties and failure mechanisms of sandwich panels with ultra-lightweight three-dimensional hierarchical lattice cores*. International Journal of Solids and Structures, 2018. **132-133**: p. 171-187.
11. Li, T., et al., *Exploiting negative Poisson's ratio to design 3D-printed composites with enhanced mechanical properties*. Materials & Design, 2018. **142**: p. 247-258.
12. Sun, Y., et al., *Bending behavior of composite sandwich structures with graded corrugated truss cores*. Composite Structures, 2018. **185**: p. 446-454.
13. Li, T. and L. Wang, *Bending behavior of sandwich composite structures with tunable 3D-printed core materials*. Composite Structures, 2017. **175**: p. 46-57.
14. EOS, *PA2200 Material data sheet*. 2019.
15. Stratasys, *PolyJet Materials Data Sheet*, Stratasys, Editor. 2019.
16. Smiths, *3003 Aluminium technical Datasheet*. 2019.
17. Bilge, K. and M. Papila, *10 - Interlayer toughening mechanisms of composite materials*, in *Toughening Mechanisms in Composite Materials*, Q. Qin and J. Ye, Editors. 2015, Woodhead Publishing. p. 263-294.